Performance Analysis of Stepped-Slot Antenna for Wireless Aeronautical Communication Services

Michael F. Adaramola[1*]   Emmanuel B. Balogun[2]

1. School of Engineering, Lagos State Polytechnic, Ikorodu, P.M.B. 21,606, Ikeja. Lagos State, Nigeria
2. Faculty of Education, Science Technology and Mathematics, University of Canberra, Australia

Abstract

This paper extensively studies the design, construction and operation of a broadband printed slot antenna. In this research work, the coplanar waveguide (CPW)-fed conventional rectangular slot antenna is designed and then the rectangular shape is modified by a stepped configuration to achieve higher bandwidth for both transmission and reception. The paper explains that the signal transmitted or received by the antenna is in the ultra wide radio frequency band. The mathematical analyses of the magnetic vector potential from the short slot were used to evaluate the total current distribution on the entire stepped-slot. The simulated results using Integrated Electronics with three-dimensional graphical output display (IE3D) software are verified by measurement and the results show that the printed stepped-slot antenna can be used for ultra wide band (UWB) communication in the frequency range of 3.1GHz – 5.7GHz. The performance and effectiveness of the printed-slot antenna finds its applications in radar antennas used with modern aircraft.

Keywords: Stepped-slot antenna, broadband, coplanar waveguide, bandwidth, Ultra wide-band communication, aircraft

1.0   Introduction

Antennas constitute a decisive component of all communication equipment and devices. It is a device used to transform an RF signal, travelling in a conductor, into an electromagnetic wave in free space (transmit mode), and to transform an RF electromagnetic wave into an electrical signal (receive mode).The choice of antenna is very important for a transmitting - receiving communication system. The antenna must be able to radiate or receive efficiently so the power supplied is not wasted. Mobility, bandwidth demands, gain and radiation efficiency as well as low cost and simple integration are requirements that need to be met. In cases where conformity is also a prerequisite, Slot antennas prove to be optimal solutions. In this context, the application of a slot antenna in wireless communications is discussed. The simulation and the measurement results show that the slot antenna provides efficient radiation pattern while being light-weight, low-cost and simple to manufacture and integrate. The subject of small antenna has attained significant attention in the recent years, because of an exorbitant demand for mobile wireless communication systems. The need for antenna miniaturization stems from the fact that most mobile platforms have a limited space for all of the required antennas in our world of ever increasing wireless systems. Compact antennas are needed so that more antennas can be closely packed together without the risk of mutual and parasitic coupling between them. For local area networks, there is an emerging interest in making antennas very small enough to ultimately fit on a single chip with the rest of the receiving front-end. At low frequencies (HF–VHF), miniature antennas are in high demand but the actualisation has become practically impossible. Since the antenna size often imposes a significant limitation on the overall size of a portable wireless system, the miniature type becomes inevitable in [1].

Section 2.0 of this paper briefly discussed the background and theoretical frameworks associated with radiation mechanism in Slot antenna. The analyses of slot and dipole current distribution were explained in section 3.0. Section 4.0 narrates the Slot antenna design and construction while section 5.0 sufficiently described the geometry of the printed stepped-slot antenna. Section 6.0 clearly describes the performance parameters and results obtained for the broadband stepped-slot antenna. Finally, the conclusions were enumerated in section 7.0.

2.0   Background and Theoretical Frameworks

The slot antenna was invented in 1938 by Alan Dower Blumein, while he was working on electromagnetic interference (EMI) and propagations. He invented it in order to produce a practical type of antenna for VHF television broadcasting that would have horizontal polarization, an incomplete omni-directional with horizontal radiation pattern and a narrow vertical radiation pattern. A slot antenna consists of a metal surface, usually a flat plane, with a hole or slot cut into it. When the plate is driven as an antenna by a driving frequency, the slot radiates electromagnetic waves in a similar way to a simple dipole antenna. The shape and size of the slot, as well as the driving frequency determines the current and radiation distribution pattern. Slot antennas are typically used at UHF and microwave frequencies when greater control of the radiation pattern is required. The slot antenna is popular because it can be cut out of whatever surface it is to be mounted on, and have radiation patterns that are roughly omni-directional (similar to a linear wire antenna) and are used typically at frequencies between 300MHz and 24GHz. The polarization of a slot antenna is typically linear. The slot size, shape, and type of material inside the

cavity of the cut-out antenna, offer design variables that can be used to tune its parameters. Slot antennas are widely used in radar antennas, for the sector antennas, for cell phone base stations, and are often found in standard desktop microwave sources. A slot antenna's main advantages are its size, design simplicity, robustness, and convenient adaptation to mass production using PC board technology. The slot antennas have the advantage of being able to produce bidirectional radiation patterns with higher bandwidth. Consider an infinite conducting sheet, with a rectangular slot cut out of dimensions length, a and width, b as shown in figure 1, if we can excite some reasonable fields in the slot (often called aperture) we have a slot antenna described by [2], [3] and [4].
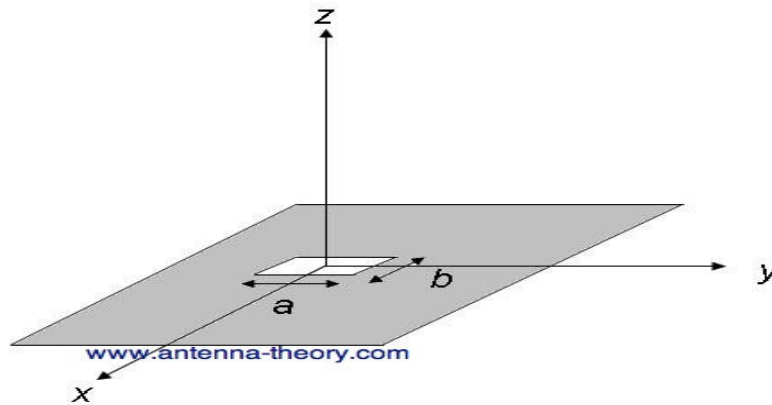

Fig. 1: The Dimensions of Slot Antenna

To gain an intuition about slot antenna, first we'll learn from Babinet's principle put into antenna terms by H.G Booker in 1946. This principle relates the radiated fields and impedance of an aperture or slot antenna to that of the field of its dual antenna. The duality of a slot antenna would be analysed if the conductive material and air were interchanged (i.e. the slot antenna become a metal slab in space). An example of dual antenna is shown in the fig. 2 below
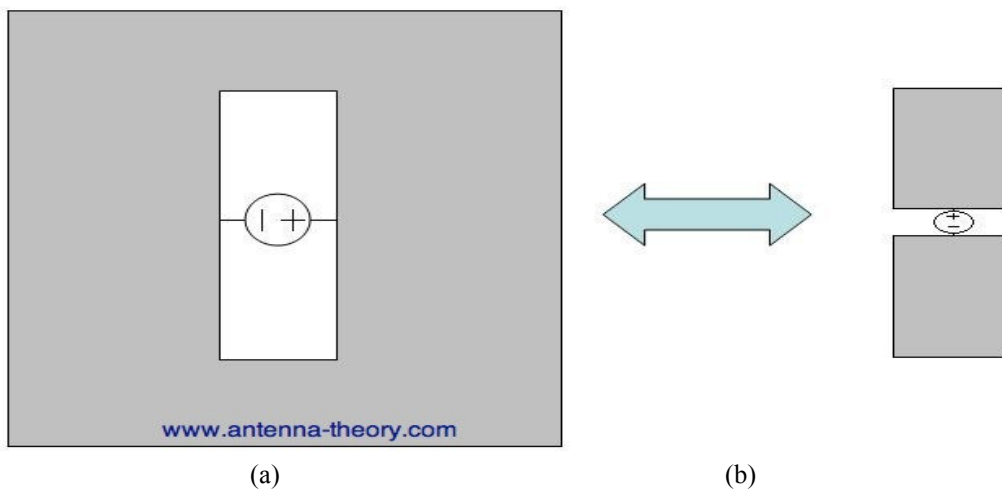

| (a)   (b) |

Fig. 2: Dual antennas-
    (a)   (left) with the slot antenna
    (b) (right) the dipole antenna

This induces an E-field distribution within the slot, and currents that travel around the slot perimeter both contributed to the radiations and its pattern. The dual antenna is similar to a dipole antenna. The voltage source is applied at the centre of the dipole, so that the voltage source is rotated. Babinet's principle relates these two antennas. The first result states that the impedance of the slot antenna (Z_S) is related to the impedance of its dual antenna (Z_C) by the relation

$$Z_C Z_S = \frac{\eta^2}{4}$$

In the above, ŋ is the intrinsic impedance of free space. The second major result   of Babinet's and Booker's principle is that the fields of the dual antenna are almost the same as the slot antenna (the fields components are interchanged, are called "duals"). That is, the fields of the slot antenna (given with a subscript s) are related to the

fields of its complement (given with a subscript c) by:

$$E_{\theta S} = H_{\theta C}$$

$$E_{\varphi S} = H_{\varphi C}$$

$$H_{\theta S} = \frac{-E_{\theta C}}{\eta 2} \quad \text{and}$$

$$H_{\varphi S} = \frac{-E_{\varphi C}}{\eta 2}$$

Hence, if we know the fields from one antenna, we know the fields of the other antenna. Hence, since it is easy to visualize the fields from a dipole antenna, the fields and impedance from a slot antenna can become intuitive if Babinet's principle is fully understood. Note that the polarization of the two antennas is reversed. That is, since the dipole antenna on the right in figure 2 is vertically polarized, the slot antenna on the left will be horizontally polarized as in [2], [3] & [4].

3.0 Analysis of Slot and Dipole Current Distribution
A thin slot in an infinite ground plane is the complement to a dipole in free space. This was described by H.G.Booker1, who extended Babinet's Principle 2,3 from optics to show that the slot will have the same radiation pattern as a dipole with the same dimensions as the slot, except that the **E-** and **H-**fields are swapped, the slot is a magnetic dipole rather than an electric dipole. The principle clearly states that the sum of the field taking separately beyond any two complimentary absorbing screens will add up to produce the field that would exist there without any screen. The interpretation of this is given as:
$U_1 + U_2 = 1$
As a result, the polarization is rotated 90º, so that radiation from a vertical slot is polarized horizontally. For instance, a vertical slot has the same pattern as a horizontal dipole of the same dimensions; and we are able to calculate the radiation pattern of a dipole. Thus, a longitudinal slot in the broad wall of a waveguide radiates just like a dipole perpendicular to the slot as shown in figure 3 below as in [4].
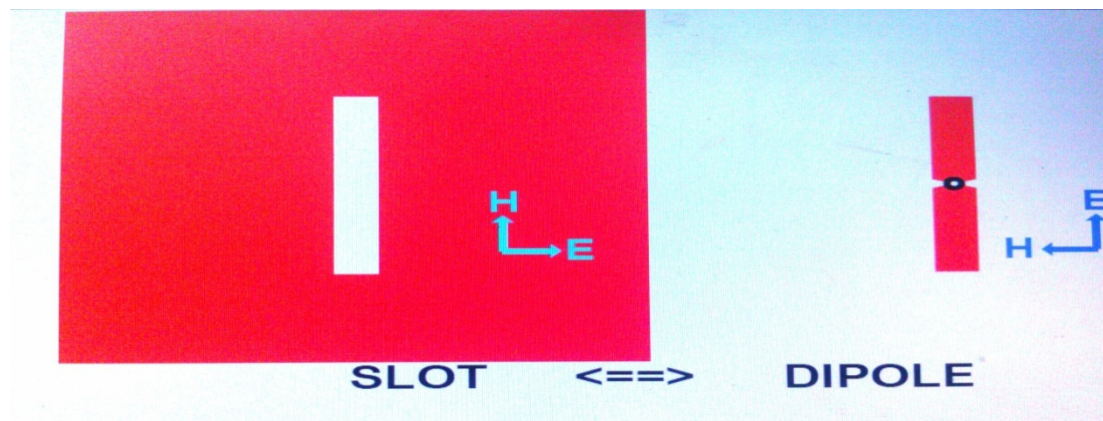

Fig. 3: Duality Example
Considering a short slot located in z-plane with a magnetic vector potential at point, P in Fig. 4 below.
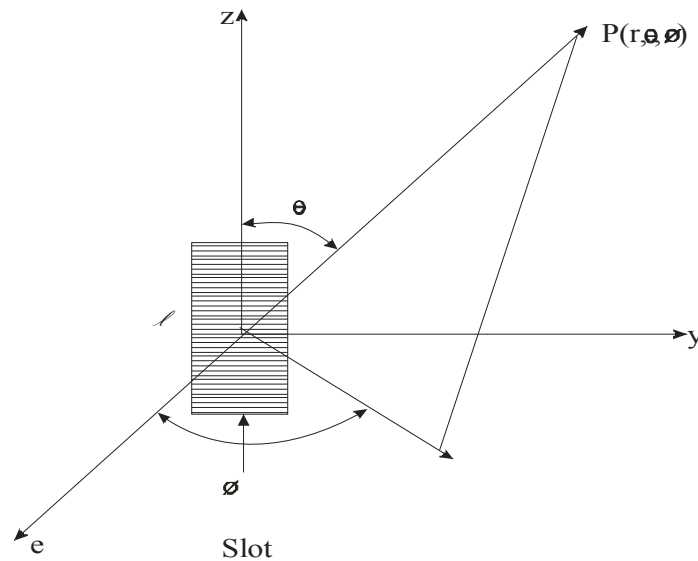
Fig.4: The Current Distribution of a Short Slot Antenna

The conjugate of the magnetic vector potential is written as:

$$A^* = \frac{E}{4\pi r} e^{-jkr} \int \int_{s'} e^{Jkr' Cos\theta} \, ds' \qquad \text{........................... 1.1}$$

$^{But} J^* = -(\acute{a}_n \, x \, \bar{E})$ (i.e. the magnetic current developed)

For the short slot conductor along the z-axis, we have the followings:

$$\hat{a}_z = \hat{a}_z \, x \, \hat{a}_y$$

$$J^* = -(\hat{a}_z \, x \, \bar{E}) \qquad \text{.. 1.2}$$

But $\bar{E} = E_0 e^{jwt}$

$$\bar{J}^{*p} = -\hat{a}_z E_0 e^{jwt} \qquad \text{…………….. 1.3}$$

$$\bar{J}^{*i} = -\hat{a}_z E_0 e^{-jwt} \qquad \text{…………….................................... .1.4}$$

Total magnetic current, J_T could be written as:

$$J_T^* = \bar{J}^{*p} + \bar{J}^{*i} = -\hat{a}_z E_0 e^{jwt} + \left(-\hat{a}_z E_0 e^{-jwt}\right)$$
$$= -\hat{a}_z E_0 \left(e^{jwt} + e^{-jwt}\right)$$
$$J_T^* = -\hat{a}_z E_0 [\cos wt + j \sin wt + \cos wt - j \sin wt] \qquad \text{........1.5}$$

Let wt $=\theta$. Therefore, the total magnetic current could be expressed as

$$J_T^* = -\hat{a}_z E_0 (2 \cos \theta)$$

The physical & imaginary field are 180^0, the total magnetic current now becomes:

$$J_T^* = -\hat{a}_z E_0 2cos \, 180^0 = -\hat{a}_z E_0 (-1)$$

$$J_T^* = \widehat{a}_z 2E_0 \quad \text{...} 1.6$$

Substituting equation (5) into (1) we have,

$$\text{A*} = \int \int_{s'} \frac{\in e^{-jkr}}{4\pi r} (\widehat{a}_z 2E_0) e^{jkr' \cos\theta} ds'$$

But r' = 0 (i.e. the position of the slot)

$$\text{A*} = \frac{\in e^{-jkr}}{4\pi r} (2E_0) \int \int_{s'} e^0 \, ds'$$

$$A_z^* = \int \int_{s'} \frac{\in e^{-jkr}}{4\pi r} (\widehat{a}_z 2E_0) e^{jkr' \cos\theta} ds' \quad \text{..................} 1.7$$

Since it is along the z-axis with a limit from $\frac{-L}{2}$ to $\frac{L}{2}$

$$A_z^* = \frac{2\in e^{-jkr}}{4\pi r} \iint dz$$

$$A_z^* = \frac{2E e^{-jkr}}{4\pi r} [z] \, _{-L/2}^{L/2} \quad \text{.....................................} 1.8$$

$$A_T^* = \frac{E e^{-jkr} 2E_0}{4\pi r} \left[\frac{L}{2} + \frac{L}{2}\right]$$

$$A_T^* = \frac{2\in E_0 L e^{-jkr}}{4\pi r} \quad \text{...} 1.9$$

Recall that $H = \frac{1}{\mu} \nabla \times \overline{A}$

And $\overline{E} = \frac{1}{E} \nabla \times A^*$

Also, $A_r = A_z \cos\theta$ and $A_\theta = -A_z \sin\theta$

$$\nabla \times \overline{A} = \begin{vmatrix} \frac{Ar}{r^2 \sin\theta} & \frac{A\theta}{r \sin\theta} & \frac{A\emptyset}{r} \\ \delta/\delta r & \delta/\delta\theta & \delta/\delta\emptyset \\ A_r & A_\theta & r \sin\theta \, A_\emptyset \end{vmatrix} \quad \text{....................} 1.10$$

$$\nabla \times \overline{A} = \frac{\breve{A}r}{r^2 \sin\theta} \left[\frac{\delta}{\delta\theta} r \sin\theta \, A_\emptyset - \frac{\delta}{\delta\emptyset} r A_\theta\right] - \frac{\widehat{a}\theta}{r \sin\theta} \left[\frac{\delta}{\delta\theta} (r \sin\theta \, A_\emptyset) - \right.$$

$$\frac{\delta Ar}{\delta \emptyset}\Bigg] + \frac{\breve{A}\emptyset}{r}\left[\frac{\delta}{\delta r}\,(rA_\theta) - \frac{\delta Ar}{\delta \theta}\right]$$

$$\nabla \times \overline{A} = \frac{\breve{a}\emptyset}{r}\left[\frac{\delta r}{\delta r}\,(rA_\theta) - \frac{\delta Ar}{\delta \theta}\right]; \ \ \text{Recall } \overline{E} = \frac{1}{E}\,\nabla \times A^*$$

But $E_0 = \dfrac{1}{E}\dfrac{\breve{a}\emptyset}{r}\left[\dfrac{\delta r}{\delta r}\,A_\theta - \dfrac{\delta Ar}{\delta \theta}\right]$

$$E_0 = \left[\frac{1}{r}\left(\frac{-2\in E_0 L e^{-jkr}}{\frac{1}{E}4\pi r}\right)\sin\theta - \frac{\delta}{\delta r}\left(\frac{2\in E_0 L e^{-jkr}}{4\pi r}\right)\cos\theta\right]$$

$$=\frac{1}{E}\left[\frac{(-jk)-2\in E_0 L e^{-jkr}}{4\pi r}\sin\theta - \frac{2\in E_0 L e^{-jkr}(-\sin\theta)}{4\pi r^2}\right]$$

$$=\frac{1}{E}\left[\frac{jk2\in E_0 L e^{-jkr}}{4\pi r}\sin\theta + \frac{2\in E_0 L e^{-jkr}(\sin\theta)}{4\pi r^2}\right]$$

$$=\frac{2\in E_0 L e^{-jkr}}{4\pi}\left[\frac{jk}{r} + \frac{1}{r^2}\right]\sin\theta$$

$$E_\theta = \frac{E_0 L e^{-jkr}}{4\pi}\left[\frac{jk}{r} + \frac{1}{r^2}\right]\sin\theta \ \ \ldots\ldots\ldots\ldots\ldots\ldots\ldots\ldots\ldots 1.11$$

At far-field, $\dfrac{1}{r^2} = 0$ (i.e. at the Fraunhofer region)

$$E_\theta = \frac{E_0 L e^{-jkr}}{2\pi}\left(\frac{jk}{r}\right)\sin\theta \ \ \ldots\ldots\ldots\ldots\ldots\ldots\ldots\ldots 1.12$$

$$E_\theta = \frac{jk E_0 L e^{-jkr}}{2\pi r}\,\sin\theta$$

But $V_0 = \hat{a}_n E_0$

$$E_\theta = \frac{jk V_0 L e^{-jkr}}{2\pi r}\,\sin\theta \ \ \ldots\ldots\ldots\ldots\ldots\ldots\ldots\ldots 1.13$$

But $\eta_0 = \dfrac{E_\theta}{H\emptyset}$

$$H_\theta = \frac{E_\theta}{\eta_0} = -\frac{jk V_0 L e^{-jkr}}{2\pi r \eta_0}\,\sin\theta \ \ \ldots\ldots\ldots\ldots\ldots\ldots\ldots 1.14$$

Equations 1.13 and 1.14 fully analyses the current distribution of this antenna as in [5], [6], [7] and [8]. As an example, consider a dipole similar to the one shown on the right in Fig.3 above. Suppose the length of the dipole is 14.4cm and the width is 2cm and the impedance at 1GHz is 65+j15Ω. The fields from the dipole antenna are given by:

$$E_{\Theta d}=E_o sin\theta$$

Using Babinet's principle, the impedance can easily be found;

$$Z_s = \eta^2/4Z_D = (120\pi)^2/4(65+J15)$$
$$Z_s =519 - j120 \ \Omega$$

From the comparative analysis of Slot and Dipole, we understand that the impedance of the slot for this case is much larger than that of Dipole. Also, the dipole's impedance is inductive (positive imaginary part) while the slot's impedance is capacitive (negative imaginary part). The E-fields for the slot can be easily found in equation 1.12, it simplifies to the following: $E_{\Phi d}=E_o sin\theta/\eta$

We see that the E-fields only contain a phi (azimuth) component making the slot antenna   to be horizontally polarized in [9] and [10].

4.0 Slot Antenna Design and Construction

Mathematical Analysis of the research work is critical to the design of the Slot antenna. The configuration of the slot printed antenna is shown with length= 88mm, width=45mm, substrate (FR4) thickness, h = 1.6 mm, dielectric constant $\varepsilon_{r\pi}$ = 4.4. Assuming practical micro-strip slot antenna substrate length and width are 110 mm for efficient radiation and using the equation stated by [2], we have:

$$F_r =c/2w\sqrt{2/(1+E_r)}$$

Width of the patch (w):

$$W = \frac{c}{2f_0\sqrt{\frac{\varepsilon_r+1}{2}}}$$

Where, c = velocity of light in free space. Using the following equation in [2] we determined the practical length L (=54mm).

$$L=L_{eff} - 2\Delta L$$

Where, the extended length of Slot antenna is heuristically deduced as:

$$\Delta L = 0.421h\frac{(\varepsilon_{reff}+0.3)(\frac{W}{h}+0.264)(}{(\varepsilon_{reff}-0.258)(\frac{W}{h}+0.8)(}$$

Effective dielectric constant of Slot antenna is expressed as:

$$\varepsilon_{reff} = \frac{\varepsilon_r+1}{2} + \frac{\varepsilon_r-1}{2}\left[1 + 12\frac{h}{W}\right]^{\frac{-1}{2}}$$

Effective dielectric length of Slot antenna is given as:

$$L_{eff} = \frac{c}{2f_0\sqrt{\varepsilon_{reff}}}$$

Where: L_{eff} = Effective length of the patch

$\Delta L/h$ =Normalized extension of the patch length

ε_{reff} = Effective dielectric constant.

The Voltage Standing Wave Ratio (VSWR) of Slot antenna is expressed as:

VSWR= V_{max}/V_{min} = (1 + /r/) ÷ (1 - /r/)

As the reflection coefficient ranges from 0 to 1, the VSWR ranges from 1 to ∞

A simple way to estimate the gain of a slot antenna is to remember that it is an array of dipoles. Each time we double the number of dipoles; we double the gain, or add 3dB. Thus, a 16 slot array would have a gain of about 12dBd. The approximate gain formula is thus given as:

Gain, A_P = 10log (N) dB; where: N is total number of slots.

Since it is really the vertical aperture of the slots rather than just the number of slots that determine the gain and vertical beamwidth of the slot antenna described in [9], [10], [11], [12], [13], [14] and [15].

5.0 Geometry of the Printed Stepped-Slot Antenna

The total length of slot (L1+L2) is 80mm, whereas L1 = L2, and the width of the slot at extreme ends (H1 = H2) is 10.5mm (See Fig.5). The gap (W2) and the width of the centre strip (W1) are 0.5mm and 2.4mm respectively. The total length of the antenna (L) is 88mm and the width of the antenna (W) is 45mm. Lengths H3, H4 and H5 are 15mm, 11mm and 7mm respectively. L3 and L4 are 20mm and 8mm respectively. The length of the CPW line (H3) is 15mm. In order to reduce the overall size of the antenna, in two corners of the patch, saw-tooth geometry of 3 mm was produced in Fig.5.
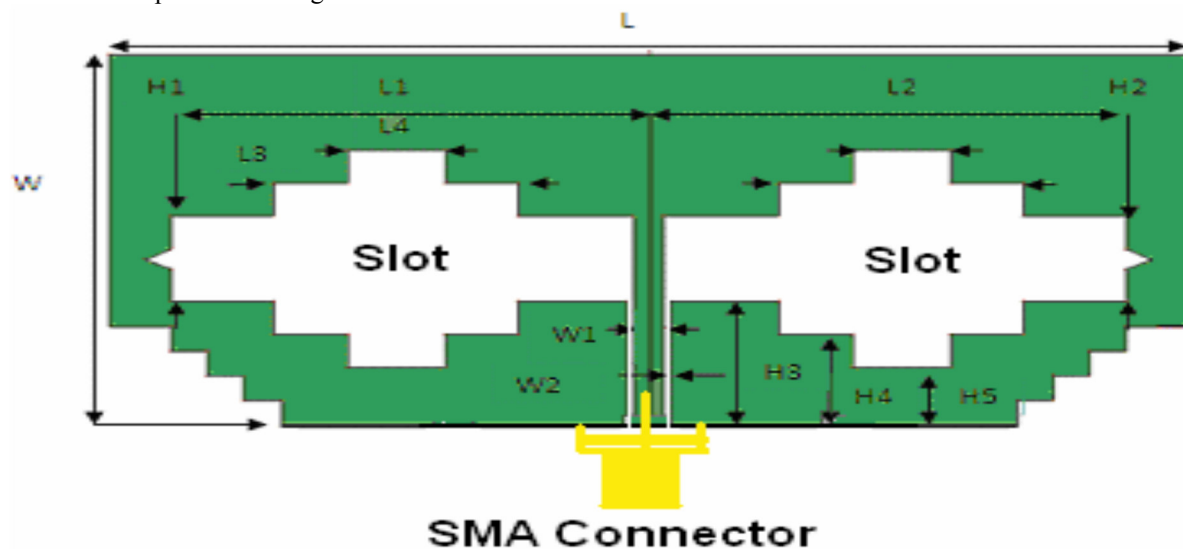
Fig. 5: Geometry of Stepped-Slot Antenna

Cutting four or two corners of the antenna smoothly, size reduction is possible but the performance of the antenna parameters degrades. Two small triangular-shaped slot extensions are used for good impedance matching without which it was not possible to achieve –10dB return loss in the frequency band of 3.1GHz – 5.7GHz. Due to these two small triangular-shaped slot extensions, other properties of antenna do not change. The dimensions of the arms of the triangles are 2mm each. The Glass Epoxy substrate of dielectric constant 4.36, height 1.57 mm, loss tangent 0.01 was used for the simulation and fabrication of the antenna. The simulated radiation patterns, antenna efficiency of the slot antenna are shown in Fig.7, Fig.8 and Fig.9 respectively. The radiation patterns are bi-directional and linearly polarized. In Fig.7 and Fig.8, the frequency difference is about 1.9 GHz. The radiation patterns of a simple dipole antenna are different for different lengths of the dipole (in terms of wavelength λ). In the present structure also the lengths of the radiating edges become different (in terms of wavelength λ) at different frequencies and therefore, radiation patterns at Fig.7 and Fig.8 are different as shown in section 6.0.

6.0 Performance Results of the Broadband Stepped-Slot Antenna

For the proposed antenna design, IE3D simulation software is used, which is a full wave electromagnetic simulation software designed for the microwave and millimetre wave integrated circuits. The primary formulation of the IE3D software is an integral equation obtained through the use of Green's function. The simulation using IE3D, takes into account, the effect of co-axial SMA connector, by which the antenna was fed. First, the simulation was started with a CPW-fed rectangular slot antenna, like Fig.1. Then in order to achieve broad bandwidth, the rectangular slot is modified to rectangular stepped-slot. The best performance of the antenna was obtained after a large number of simulations where dimensions of stepped slot (L1, L2, L3, L4, W1, W2, W3, W4, H1, H2, H3, H4) width of the feed strip (W2) and dimensions of the radiating patch (L, W), are varied to achieve the maximum bandwidth (in terms of impedance bandwidth and gain) of the antenna. The fabricated antenna prototype is shown in Fig.6.

Fig.6: Stepped-slot Antenna Prototype Unit

The simulated radiation patterns, antenna efficiency of the slot antenna are shown in Fig.7, Fig.8, and Fig.9 respectively. The radiation patterns are bi-directional and linearly polarized. In Fig.7 and Fig.8, the frequency difference is about 1.9 GHz. The radiation patterns of a simple dipole antenna are different for different lengths of the dipole (in terms of wavelength λ). In the present structure also the lengths of the radiating edges become different (in terms of wavelength λ) at different frequencies and therefore, radiation patterns at Fig.7 and Fig.8 are different which follows the similar pattern in [14] and [15].
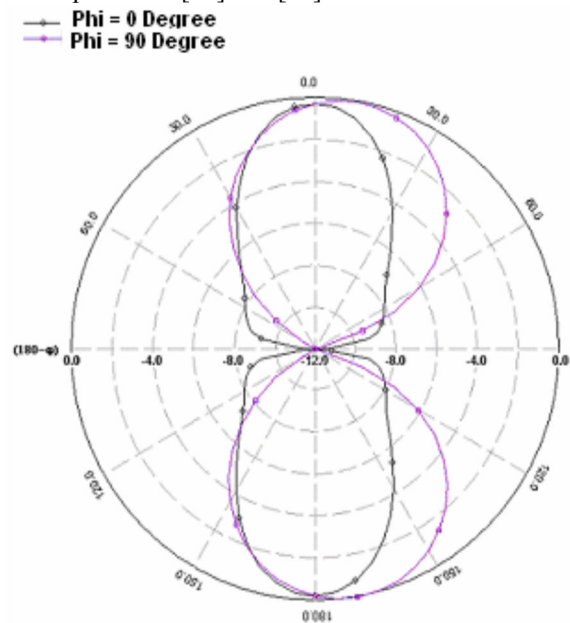
Fig. 7: Radiation Pattern at 3.63GHz
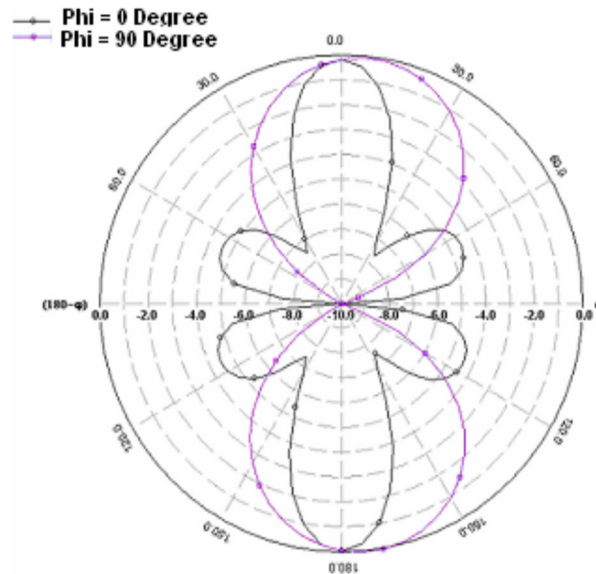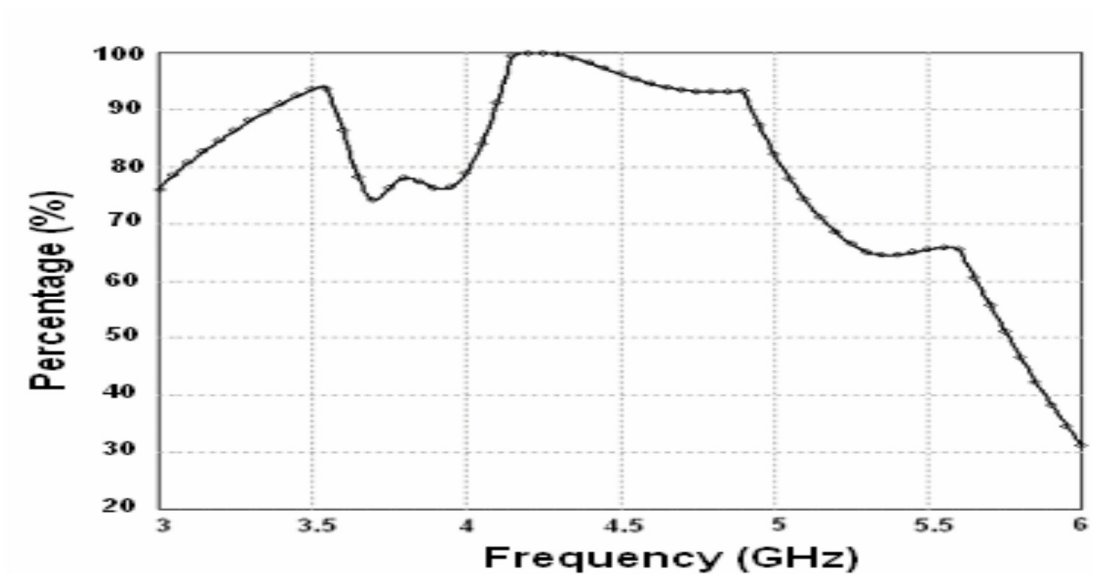
Fig. 8: Radiation Pattern at 5.4GHz

Fig.9: Percentage Directive Gain versus Frequency Bandwidth.

After fabrication of the antenna, measurement was done using vector network analyser (VNA N5230A of Agilent Technologies). The simulated and measured return losses of the antenna are compared in Fig.10. The real (R_{in}) and imaginary parts (X_{in}) of the input impedance are plotted in Fig. 8. The simulated and measured gains of the antenna are compared in Fig.11. The maximum simulated gain of the antenna is 6.5dB and minimum gain is 2.4dB over the frequency range of 3.1 – 5.7GHz. The gain of the antenna was measured at discrete frequencies over the band of the antenna.
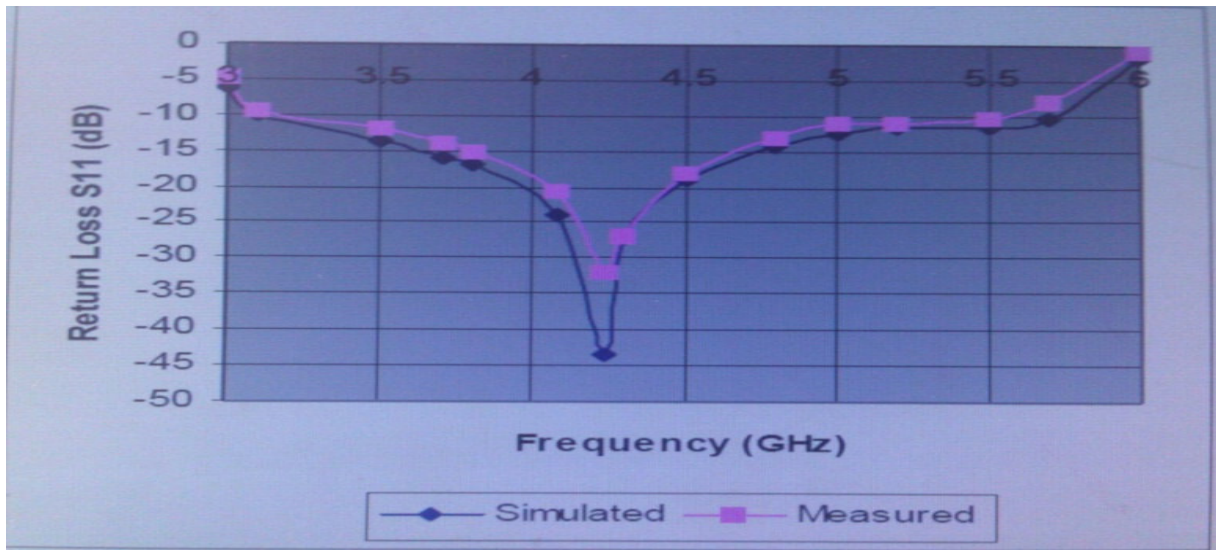
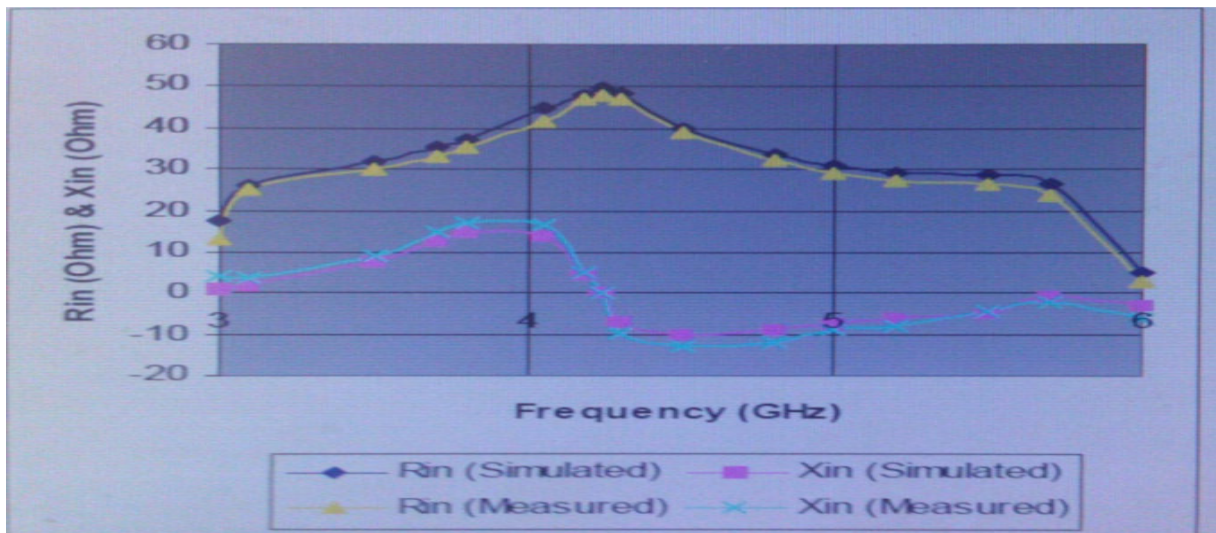Fig. 10: Comparison between Simulated and Measured Return Losses (S11)

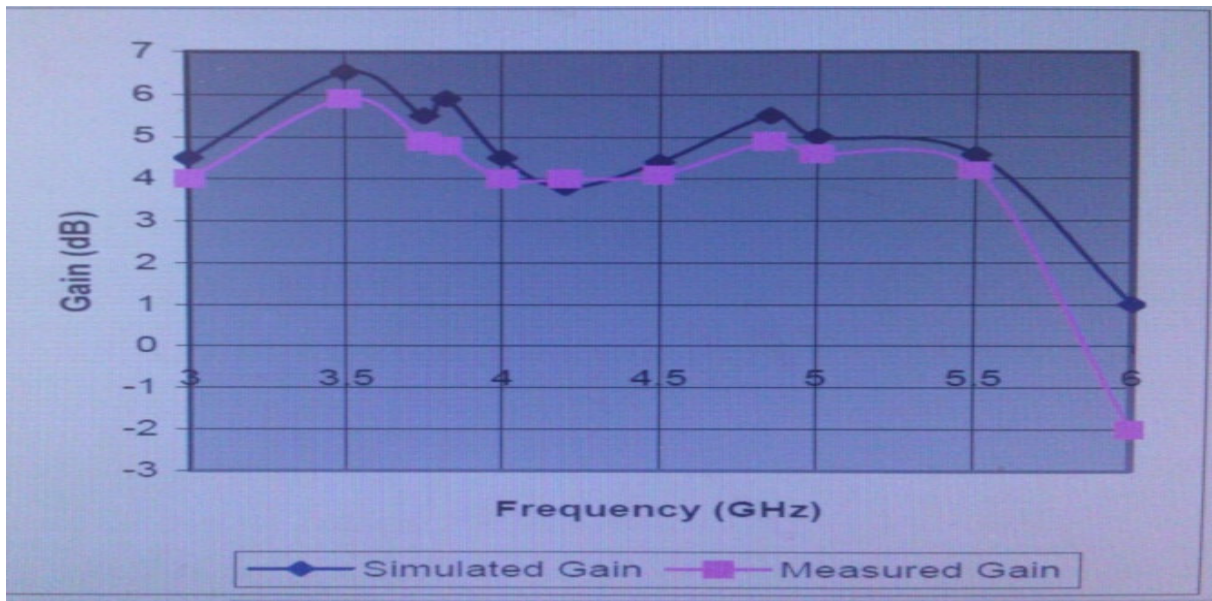Fig. 11: Real (R_{in}) and Imaginary (X_{in}) Parts of Input Impedance of the Antenna

Fig.12: Comparison between Simulated and Measured Gains

For gain measurement, two identical antennas were fabricated (as shown in Fig.6) and transmission coefficient S12 was measured using vector network analyser without using anechoic chamber. Separation between the two antennas is noted. By using Friis transmission formula, the directive gain of the antenna was determined. The schematic set up for the measurement of gain using vector network analyser is shown in Fig. 13.
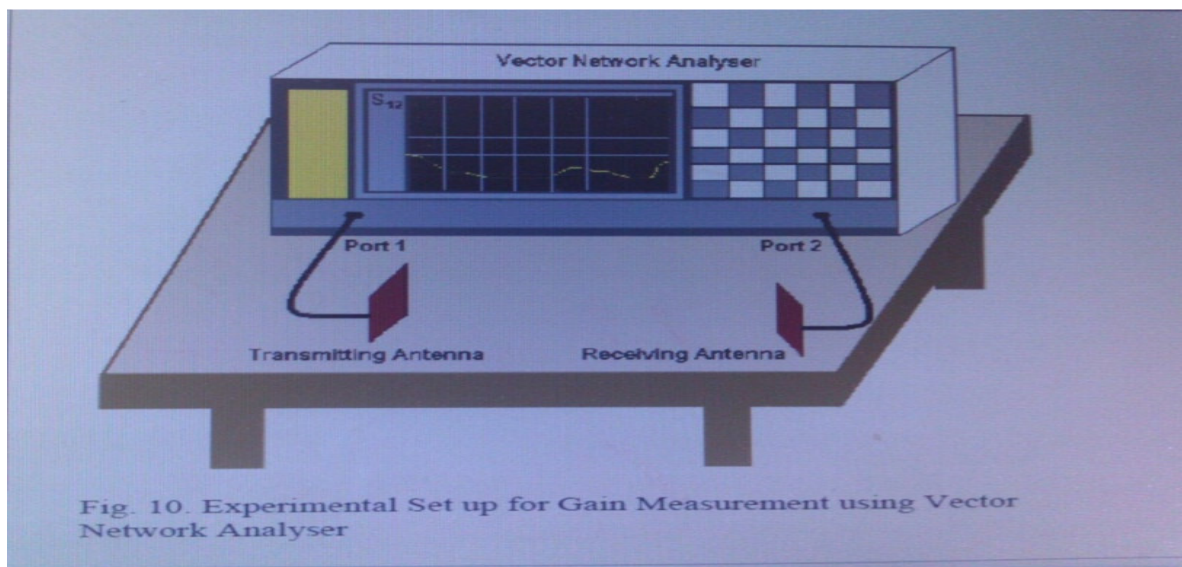

Fig. 10. Experimental Set up for Gain Measurement using Vector Network Analyser

Fig. 13: Vector Network Analyser

Constant group delay is one of the required characteristics of UWB antenna. Measured Group delay, when the separation between two antennas is 45 cm, is shown in the graph of Fig.14. The average group delay is approximately 2ns. Group delay is nearly constant over the frequency bandwidth from the graph in [16] & [17].
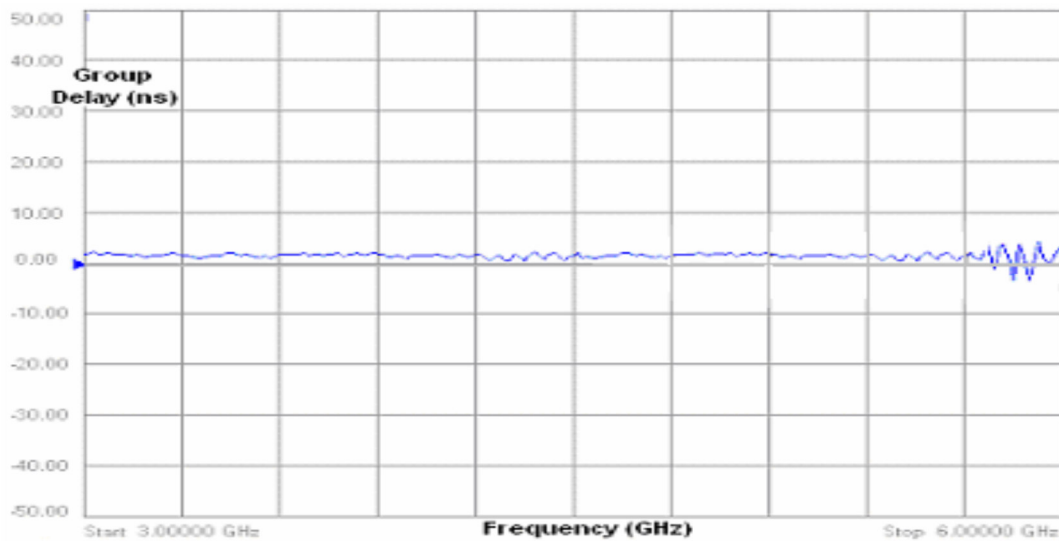
Fig. 14: Graph of Group Delay versus Frequency Bandwidth.

From fig. 11, it clearly shows that in some places group delay could be negative (i.e. transmitting frequency near 6GHz). Group delay is determined from the slope (dΦ/df) of the Phase versus Frequency graph of S21 parameter and expressed as τ_g = (-1/360)(dΦ/df). In a network analyzer, when calibration is done over a wide range of frequency (specially, if the frequency band is more than 1GHz), calibration becomes inaccurate. Due to inaccurate calibration, the slope of the phase-frequency curve (dΦ/df) becomes positive at certain frequencies and ultimately, according to above formula, τ_g becomes negative. For that reason, some parts of the measured group delay curve over a wide frequency range (here it is 2.6GHz), always show negative group delay.

7.0 Conclusion

A new broadband printed slot antenna with stepped slot is designed for the application in UWB wireless communication. The antenna has a very small size for UWB application. The in-depth analysis and results show that the directive gain of the antenna may be low (i.e. greater than 2dB), but the antenna efficiency would be high enough (i.e. greater than 60%), which is achieved by simulation and measurement from the proposed antenna over the bandwidth range. The outstanding performance and effectiveness of the printed-slot antenna finds its applications in radar antennas used with aircraft, sector antennas, cell phone base stations antennas, and standard desktop microwave sources.

8.0 References

[1] www.antennatheory.com (2015)

[2] E. S. Angelopoulos, A. Z. Anastopsoulos, D. I. Kaklamani, A. A. Alexandridis, F. Lazarakis and K. Dangakis, (2006) "Circular and Elliptical CPW-fed Slot and Micro-strip Centre-fed Antennas for Ultra wide band Applications", IEEE Antennas and Wireless Propagation Letters, vol. 5, pp. 294 – 297, 2006.

[3] G. Kumar and K. P. Ray, (2003) "Broadband Micro-strip Antennas", Artech House, Boston, 2003.

[4] C. A. Balanis (1996), "Antenna Theory: Analysis and Design", 2nd Edition, John Wiley and Sons, New York, chapter 4 section 4 & 8 USA

[5] M. Kahrizi, T. Sarkar and Z. Maricevic, (1993), "Analysis of a wide radiating slot in the ground plane of a micro-strip line", IEEE Transaction on Microwave Theory Technology, Vol. 41, pp 29-37

[6] A. A. Eldek, A. Z. Elsherbani and C. E. Smith, (2003) "Wideband bow-tie Slot antennas for radar applications" 2003 IEEE Tropical Conference on Wireless Communication Technology, Honolulu, Hawaii

[7] J. Ghosh and J. S. Roy, (2008) "Design of a Wideband Micro-strip Antenna", Journal of Electromagnetic Waves and Applications, JEMWA, vol. 22, pp. 2379-2389, 2008.

[8] J. R. James and P. S. Hall, (1989) "Handbook of Micro-strip Antennas", Vol. 1, Peter Peregrinus Ltd., London, UK, 1989.

[9] J. S. Roy and M. Thomas, (2007) "Compact and Broadband Micro-strip Antennas for Next Generation High Speed Wireless Communication Using HIPERLAN/2", International Journal of Microwave Science and Technology, pp. 1-4, 2007.

[10] J. S. Roy and M. Thomas, (2007) "Investigations on a New Proximity Coupled Dual- Frequency Micro-strip Antenna for Wireless Communication", Microwave Review, Vol. 13, No. 1, pp. 12– 15, June 2007.

[11] J. S. Roy, and M. Thomas, (2008) "Design of a Circularly Polarized Micro-strip Antenna for WLAN", Progress in Electromagnetic Research, PIER M, Vol. 3, pp. 79 – 90, 2008.

[12] K. L. Wong, (2002) "Compact and Broadband Micro-strip Antennas", John Wiley, New York, USA 2002.

[13] R. Garg, P. Bhartia, I. J. Bahl and A. Ittipiboon, (2001) " Micro-strip Antenna Design Handbook", Artech House, 2001.

[14] X. Jing, Z. Du and K. Gong, (2006) "A Compact Multi-band Planar Antenna for Mobile Handsets", IEEE Antennas and Wireless Propagation Letters, vol. 5, pp. 343 – 345, 2006

[15] D. Llorens, P. Otero and C. Camacho-Penalosa, (2003), "Dual-Band single CPW port planar-slot antenna" IEEE Transaction on Antennas and Propagation Vol. 51, pp 137-139

[16] R. N. Simons (2001), "Coplanar Waveguide Circuits, Components and Systems", John Wiley and Sons, New York, pp 1-6, 422-424, USA

[17] S. L. S. Yang, A. A. Kishk and K. F. Lee, (2008), "Frequency reconfigurable U-Slot micro-strip patch ", IEEE Antennas for Wireless Propagation Letters, Vol. 7, pp 127-129